Thin-walled Beam Bending Quartic Deplanation Analytical Function for Improved Experiment Matching

A Halim Kadarman[*], Nabilah Azinan, Junior Sarjit Singh Sidhu
School of Aerospace Engineering
Universiti Sains Malaysia, 14300 Nibong Tebal, Penang, Malaysia
[*]Email: ahalim@usm.my

Solehuddin Shuib
Faculty of Mechanical Engineering
Universiti Teknologi Mara, 40450 Shah Alam, Selangor, Malaysia

ABSTRACT

Ensuring the accuracy of an analytical solution is important in modeling real engineering structures. For determining the stress-deformation condition of a thin-walled beam structure in bending, inadequately, the simple beam formula can only provide uniform average stress-deformation distribution at specific cross-sectional elevations. The recently developed analytical solution for determining stress-deformation conditions with consideration of the shear lag effect of a prismatic thin-walled box beam subjected to transverse load causing bending using classical quadratic deplanation function did not provide an accurate but rather a good estimate when compared with finite element analysis results. In this paper, the objective of the study was to see if the accuracy can be improved. The same Vlasov's method was used. The method was developed using Calculus of Variations based on a Stress-form stationary condition complementary energy which included the shear lag effect. All calculations were computerized using the software MAPLE 18 which assisted in getting quick results (especially for preliminary design studies) for various geometries, material properties, and loading conditions. Several deplanation functions were introduced. Two variants of the quadratic functions, i.e. x^2y^3 and x^2y, and the quartic functions, i.e. x^4y^3 and x^4y were used to find the best match against empirical data and FEA (finite element analysis) results. The finding was that the quartic variant of the deplanation functions provided improved matching with experimental data as well as FEA results. Noteworthy to point

ISSN 1823-5514, eISSN 2550-164X
Received for review: 2020-08-28
Accepted for publication: 2020-12-11
Published: 2021-01-15

out that the characteristic of the functions with quartic-x or x^4 of having almost flat variation in the center part enhances matching with the experimental data. Moreover, the characteristic of the function with cubic-y or y^3 of having steeper slopes enhances matching with the FEM results at the edge.

Keywords: *Thin-walled beam bending, Deplanation function, Thickness-radius ratio, Shear lag, Analytical vs Experiment*

Introduction

Thin-walled box beams are widely used in engineering structures such as civil, mechanical, and aerospace for bridges, buildings, aircrafts, and rockets. The basic simple beam solution for determining the stress-deformation of beams in bending can only provide uniform average stress-deformation distribution at specific cross-sectional elevations which is inadequate for thin-walled beams that experience the shear lag effect. Hence, an analytical formula or calculation method which includes the shear lag effect is needed to provide a more reliable, and more accurate representative estimate of this stress-deformation condition.

The developed analytical solution in [1] based on Vlasov's method [2] for determining stress-deformation conditions with consideration of the shear lag effect of a prismatic thin-walled box beam subjected to transverse load causing bending using classical quadratic deplanation function did not provide an accurate but rather a good estimate when compared with finite element analysis results. In this paper, the objective of the study was to see if the accuracy can be further improved using the same method but only changing the deplanation/distortion functions. This Vlasov's method was developed using Calculus of Variations based on a Stress-form stationary condition complementary energy which included the shear lag effect. All calculations were computerized using the software MAPLE 18 [3] which assisted in getting quick results (especially for preliminary design studies) for various geometries, material properties, and loading conditions.

In this paper, several deplanation functions were introduced. Two variants of the quadratic functions, i.e. x^2y^3 and x^2y, and the quartic functions, i.e. x^4y^3 and x^4y were used to find the best match against empirical data and FEA (finite element analysis) results.

The finding was that the quartic variant of the deplanation functions provided improved matching with experimental data as well as FEA results. Noteworthy to point out that the characteristic of the functions with quartic-x or x^4 of having almost flat variation in the center part enhances matching with the experimental data. Furthermore, the characteristic of the function with cubic-y or y^3 of having steeper slopes enhances matching with the FEM results at the edge.

Literature background

Kadarman et al. [1] analytically developed a version of Vlasov's Stress-form using the variational method and found very close matching of the analytical Stress-form and recognized Displacement-form from [4]. Comparison with FEM showed that the Stress-form results were matching well at the high stress region and were slightly higher at the intermediate stress area.

In [5], using the variational method, both elastic and inelastic solutions were shown. Here, Lin and Zhao studied the effect of shear lag in steel box beams. The verification of the analytical method was done by experimental means of testing on steel box beams. Comparison of the proposed variation method with experimental data found that the model predicts quite well the steel box beams' plastic normal strain distribution and deflection.

In [6], using the variational principle, an analytical solution taking into account the shear lag was presented by Chen et al. Using the principle of superposition, the problem of loaded simply supported and cantilever beams were solved. The calculated normal stress was well predicted.

In this paper, an analytical method developed recently in [1] was verified further by comparison with experimental data from [5] – [8] and also by FEM. Flexural bending of a thin-walled box can cause Deplanation/Distortion due to the shear lag effect (Figure 1).

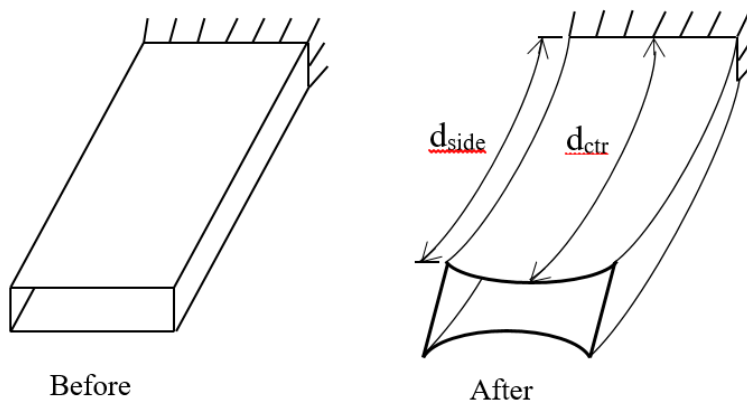

Figure 1: Box beam flexural bending causes contraction of d_{side} to differ from d_{ctr} [1].

Analytical Formulation

First Step – establishing stresses

The hollow doubly-symmetric prismatic thin-walled box beam in Figure 2 is clamped at one end and its section is centered at the origin of the x, y and, z axes. It is subjected to the transversal distributed load w_y acting through the elastic axis that causes shear $V_y = \int_0^z w_y(z)dz$ and moment $M_x = \int_0^z V_y(z)dz$. As in [1, 9] the analytical solution is derived based on these loads.

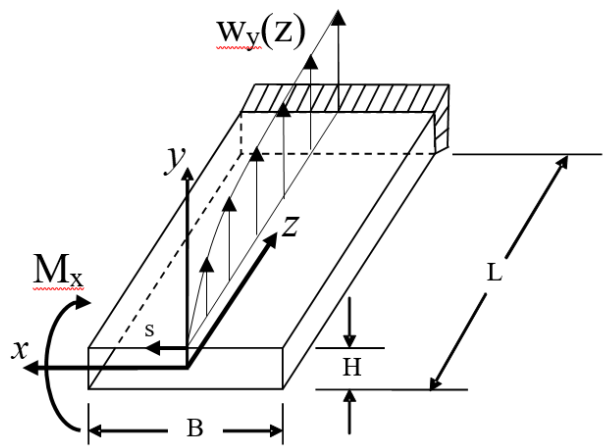

Figure 2: Hollow Box beam with distributed load w_y [1].

Using curvilinear coordinate s as in [10, 11], the equations of equilibrium similar to equations 3.90a and 3.90b in [12]:

$$\frac{\partial N_z}{\partial z} + \frac{\partial N_{zs}}{\partial s} = 0 \quad , \quad \frac{\partial N_{zs}}{\partial z} + \frac{\partial N_s}{\partial s} = 0 \tag{1}$$

From Equation (1), N_{zs} and N_s can be written in term of N_z,

$$N_{zs} = -\int \frac{\partial N_z}{\partial z} ds + q_0(z) \tag{2}$$

$$N_s = \iint \frac{\partial^2 N_z}{\partial z^2} ds^2 - \left[\int q_0'(z) ds\right] + n(z) \tag{3}$$

Let the longitudinal stress resultant, N_z be the combination of a simple beam solution and a term with the deplanation function $\overline{\varphi_4}(s)$ which shapes the stress resultant distribution due to distortion along the s-contour:

$$N_z = N_{z,SB} + X_4\varphi_4 \tag{4}$$

where $N_{z,SB} = -\frac{M_x}{I_x} y h_i$ (**S**imple **B**eam)

$X_4(z) \equiv$ deplanation intensity multiplier along z

$\varphi_4 = \overline{\varphi_4} + C_1 N_{z,SB}$, $\overline{\varphi_4} = x^2 y$ or $x^2 y^3$ or $x^4 y$ or $x^4 y^3$

$C_1 \equiv$ orthogonalization coefficient

I_x= centroidal area moment of inertia. C_1 is determined by orthogonalization of functions [13] (also see Appendix) to ensure that the resulting distribution of stress resultants self-equilibrate (self-balance) in the section to preserve force equilibrium with the simple beam uniform stress level:

$$\oint N_{z,SB}\varphi_4 \, ds = 0$$

Now continue on with N_{zs}, insert Equation (4) into Equation (2):

$$N_{zs} = -\int (N'_{z,SB} + X'_4\varphi_4)\, ds + q_0(z) \tag{5}$$

Substitute $q_Q(s,z) = -\int N'_{z,SB}\, ds$ into Equation (5) and rearrange:

$$N_{zs} = q_Q(s,z) + q_0(z) - X'_4 \int \varphi_4 \, ds \tag{6}$$

The first two terms of Equation (6) are simple beam solutions. And:

$$q_Q(s,z) = \frac{V_y Q_x^{\Delta}}{I_x}$$

is familiarly known as the shear flow that varies with the first moment of area:

$$Q_x^{\Delta} = \int_0^s \bar{y} ds$$

while $q_0(z)$ is the constant shear flow. For the analytical solution of $q_0(z)$, the torsional moment equilibrium is used:

$$M_z = \oint N_{zs}\rho ds$$

There is no torsional moment and w_y is acting through the elastic axis, hence M_z is zero:

$$0 = \oint N_{zs}\rho ds \tag{7}$$

Insert Equation (6) into Equation (7):

$$0 = \oint \left\{q_Q(s,z) + q_0(z) - X_4' \int \varphi_4 \, ds\right\}\rho ds$$

Take $q_0(z)$ out of the integral since it is independent of s and use $\omega = \oint \rho ds$:

$$q_0(z) = \frac{1}{\omega}\left[-\oint q_Q(s,z)\rho ds + X_4' \oint \left(\int \varphi_4 ds\right)\rho ds\right] \tag{8}$$

Insert Equation (8) into Equation (6) and let:

$$q_{Mz} = q_Q(s,z) - \frac{1}{\omega}\oint q_Q(s,z)\rho ds$$

and

$$b_4(s) = \int \varphi_4 ds - \frac{1}{\omega}\oint \left(\int \varphi_4 ds\right)\rho ds$$

Hence:

$$N_{zs} = q_{Mz} - X_4' b_4 \tag{9}$$

Second step – using variational calculus

Variational calculus is explained comprehensively in [14]. The analytical solution of $X_4(z)$ is obtained using the Variational Principle of the Least Work. After substituting the stresses into the Potential energy functional,

$$U = \int_0^L \Phi(X_4, X_4', z)dz$$

and minimization of this functional, a differential equation of displacement

compatibility is produced. Then after solving the differential equation and applying the boundary conditions the complete solution for N_z and N_{zs} can be obtained. In this case:

$$U = \int_0^L \left[\oint \left(\frac{N_z^2}{2Eh} + \frac{N_{zs}^2}{2Gh} + \frac{N_s^2}{2Eh} \right) ds \right] dz$$

.

N_s has relative negligible value as extensively discussed in [15], hence:

$$U = \frac{1}{2} \int_0^L \left[\oint \left(\frac{N_z^2}{Eh} + \frac{N_{zs}^2}{Gh} \right) ds \right] dz$$

Insert Equation (4) and Equation (9):

$$U = \frac{1}{2} \int_0^L \oint \left\{ C_{11} \left[N_{z,SB} + X_4 \varphi_4 \right]^2 + C_{33} [q_{Mz} - X_4' b_4]^2 \right\} ds dz$$

where $C_{11} = {}^1/_{Eh}$ and $C_{33} = {}^1/_{Gh}$. Let stress function,

$$\Phi = \frac{1}{2} \oint \left\{ C_{11} \left[N_{z,SB} + X_4 \varphi_4 \right]^2 + C_{33} [q_{Mz} - X_4' b_4]^2 \right\} ds$$

To minimize:

$$U = \int_0^L \Phi(X_4,\ X_4', z) dz$$

the Euler-Lagrange equation:

$$\frac{d}{dz} \frac{\partial \Phi}{\partial X_4'} - \frac{\partial \Phi}{\partial X_4} = 0$$

must be satisfied. Hence insert Φ and differentiate:

$$\frac{\partial \Phi}{\partial X_4'} \qquad \text{and} \qquad \frac{\partial \Phi}{\partial X_4}$$

and substitute to get:

$$\frac{d}{dz}\left\{\oint[-C_{33}(q_{Mz}-X_4'b_4)b_4]ds\right\}-\oint\left[C_{11}\left(N_{z,SB}+X_4\varphi_4\right)\varphi_4\right]ds=0$$

Continue to differentiate with respect to z,

$$\oint\left[-C_{33}\left(b_4q_{Mz}'-b_4^2X_4^{"}-2b_4b_4'X_4'+b_4'q_{Mz}\right)\right]ds$$
$$-\oint\left[C_{11}\left(N_{z,SB}+X_4(z)\varphi_4\right)\varphi_4\right]ds=0$$

And expanding:

$$\oint C_{33}b_4^2X_4^{"}ds+\oint C_{33}2b_4b_4'X_4'ds+\oint C_{11}X_4\varphi_4^2ds$$
$$=\oint C_{11}N_{z,SB}\varphi_4ds+\oint C_{33}b_4q_{Mz}'ds+\oint C_{33}b_4'q_{Mz}ds$$

As b_4 is independent of z, hence $b_4'=0$ and $X_4$and $X_4^{"}$ are independent of s, so they can be taken out of the integrations:

$$X_4^{"}\oint C_{33}b_4^2ds-X_4\oint C_{11}\varphi_4^2ds=\oint C_{11}N_{z,SB}\varphi_4ds+\oint C_{33}b_4q_{Mz}'ds$$

And simplifying, produces a second order differential equation:

$$A_{11}X_4^{"}-A_{12}X_4=B_1+B_2$$

where

$$A_{11}=\oint C_{33}b_4^2ds\quad,\quad A_{12}=\oint C_{11}\varphi_4^2ds,$$

$$B_1=\oint C_{11}N_{z,SB}\varphi_4ds\quad,\quad B_2=\oint C_{33}b_4q_{Mz}'ds$$

Derived from calculus of variations, the natural boundary condition (condition of clamping) for determining constants of the solution at $z=L$:

$$\frac{\partial\Phi}{\partial X_4'}=0\quad\rightarrow\quad\oint C_{33}\,q_{Mz}b_4ds-X_4'\oint C_{33}b_4^2ds=0\qquad(10)$$

And at $z=0$, static equilibrium boundary condition:

$$\oint N_zyds=M_x=0$$

Finite Element Modeling

For the finite element modeling, 3-D solid elements were used instead of 2-D plate elements because of the need to compare with experimental data measured at the surface which 3-D solid elements can provide direct comparative values. The FEA are limited to linear static isotropic material meaning that plastic deformation beyond yielding was not considered. Quarter models were created and analyzed using the SOLIDWORKS software 2019 Education Edition [16] to represent the simply-supported structure with symmetry boundary constraints imposed at the longitudinal and center transverse planes and fixed vertical displacement at the bottom edge of the end of the transverse plane while 25% of the full vertical load were applied at the outside edge of the center transverse plane as shown in Figure 3.

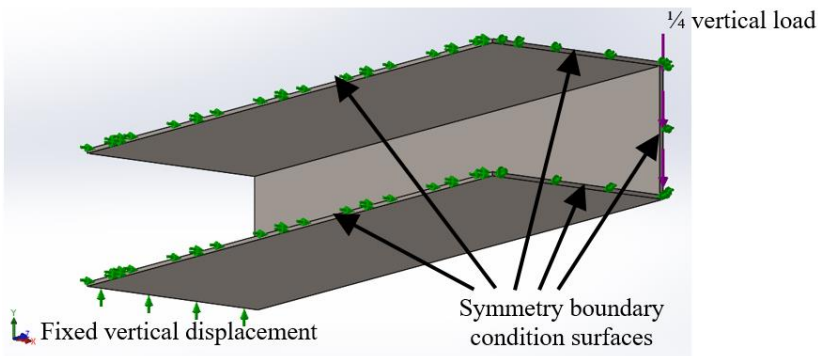

Figure 3: A sample of the Quarter FE Model (bottom view) showing how boundary conditions and load are imposed.

Comparison with Experimental Data and/or FEM

To evaluate the analytical Stress-form method developed, it was compared to existing experimental data by Ahmad stated in [5], [6], [8] and by Zhibin stated in [5], [6], [7] and newly acquired FEM results. Both Ahmad's and Zhibin's tests were conducted using simply-supported beams with measured strains at the mid-span, therefore these data were compared to the Stress-form method solutions at the fixed cantilever end to have a similar effect.

For the comparisons, the following two evaluation aspects were considered:

1. Geometry satisfying thin-walled definition. In Allen and Haisler [17]: thin-walled means a bar of circular cross- section to be one in which the

thickness t is less than or equal to 5 percent of the average radius, or $\frac{t}{r_{avg}} \leq 0.05$.

2. Matching experimental data and/or FEM results with solutions of the analytical Stress-form method using several Deplanation functions, $\overline{\varphi_4}$.

Table 1 summarized the comparisons that were done and the details are described subsequently.

Table 1: Summary of Comparisons

No.	Specimens	Comparison items	$\frac{t}{r_{avg}}$	Thin-walled?
1	300 x 100 x 3 mm	Experiment, FEM, x^4y^3, x^4y, x^2y^3 & x^2y	$\frac{3}{1/2\,(150+50)} = 0.03$	Yes
2	5 x 2 x 0.1875 in	Experiment, FEM, x^4y^3, x^4y, x^2y^3 & x^2y	$\frac{0.1875}{1/2\left(\frac{5}{2}+\frac{2}{2}\right)} = 0.107$	No
3	400 x 100 x 3 mm	FEM, x^4y^3, x^4y, x^2y^3 & x^2y	0.024	Yes
4	200 x 100 x 3 mm	FEM, x^4y^3, x^4y, x^2y^3 & x^2y	0.04	Yes

First comparison (Analytic, Data, and FEM)

The first experimental data for comparison comes originally from work done by Ahmad [5], [6], [7]. The box beam used in the experiment from Ahmad was a simply-supported beam that had a span length and cross-sectional dimensions of 1 m and 300 x 100 x 3 mm, respectively. A load of 6 kN was imposed at the mid-span as shown in Figure 4. Stresses were calculated from the strains measured at the mid-span [5]. The comparison result is shown in Figure 5.

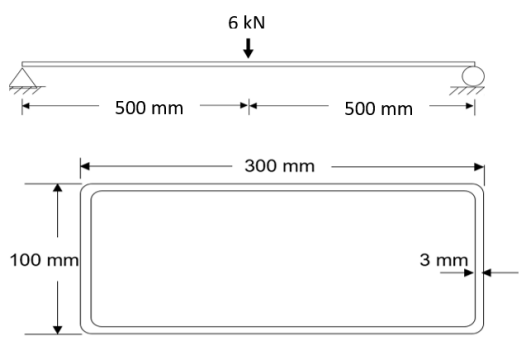

(a)

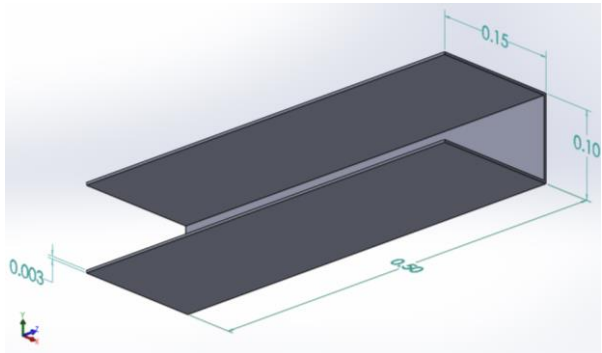

(b)

Figure 4: (a) Geometry of the Structure (b) Quarter FEM of the Structure with dimensions in meters.

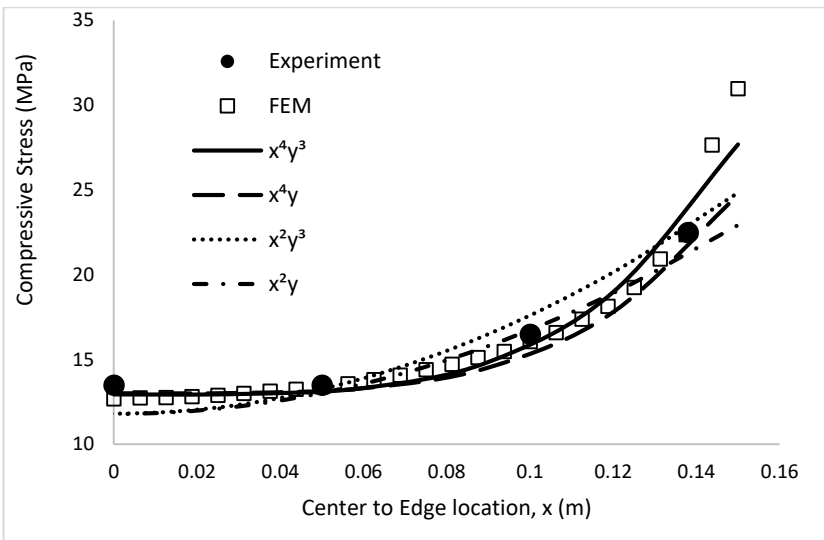

Figure 5: First Comparison of Experiment, Various Deplanation Functions, and FEM.

Second comparison (Analytic, Data, and FEM)

The second experimental data for comparison comes from a test carried out by Zhibin [5], [6]. The box beam used in the experiment by Zhibin [5], [6] was also a simply-supported beam which had a span length and cross-sectional dimensions of 21 inches (533 mm) and 5 x 2 x 3/16 inches (127 x 50.8 x 4.763

mm), respectively as shown in Figure 6. Again, at the mid-span, 45.43 kN (10.2 kips) load was imposed. And from the measured strains on the top flange's outer surface at mid-span, stresses were calculated. The comparison result is shown in Figure 7.

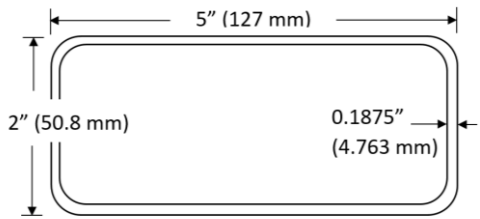

(a)

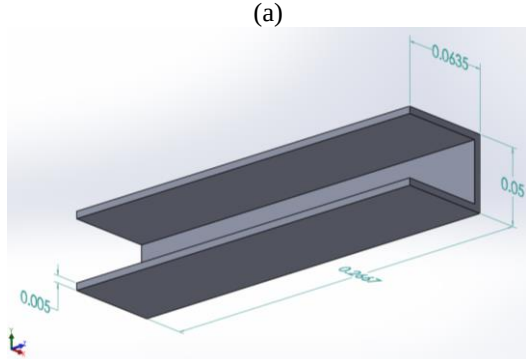

(b)

Figure 6: (a) Geometry of the Structure (b) Quarter FEM of the Structure with dimensions in meters.

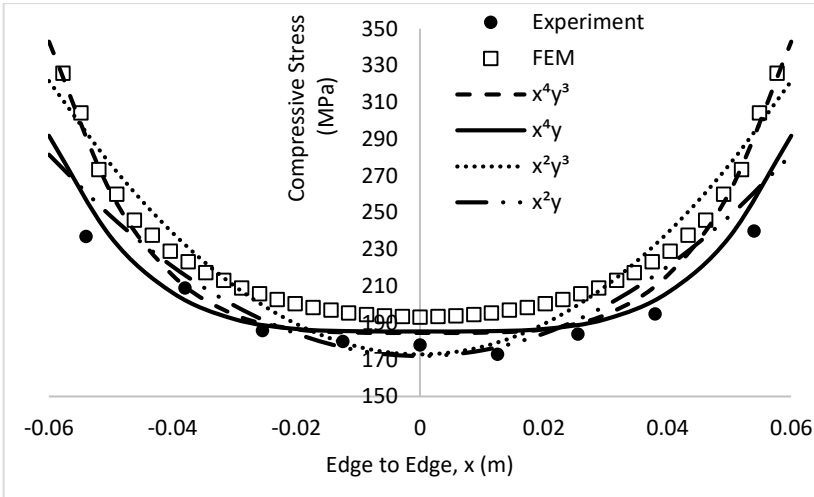

Figure 7: Second Comparison of Experiment, Various Deplanation Functions, and FEM.

Third and Fourth comparisons (Analytic and FEM only)

The third and fourth comparisons were with FEM only and also for a simply-supported beam that had the same span length and cross-sectional dimensions of 1 m and 400 x 100 x 3 mm and 200 x 100 x 3 mm, respectively. A load of 6 kN was imposed at the mid-span. The third and fourth comparison results are shown in Figures 8 and 9, respectively.

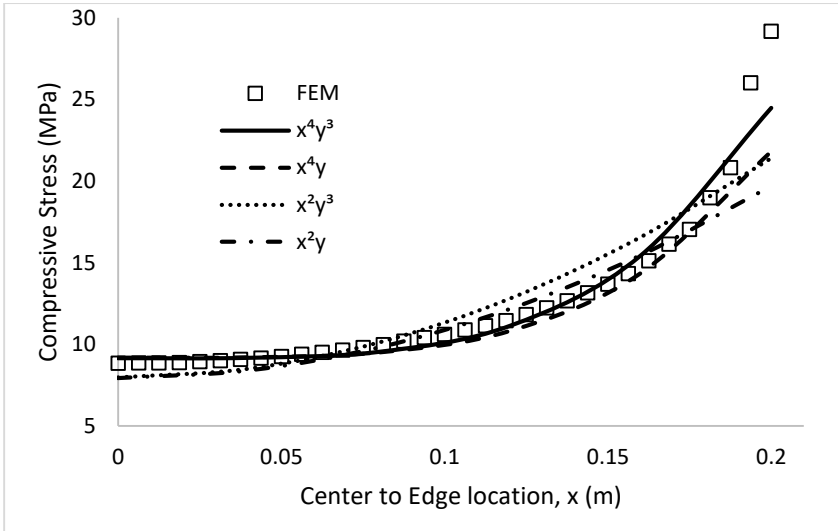

Figure 8: Third Comparison of Various Deplanation Functions, and FEM.

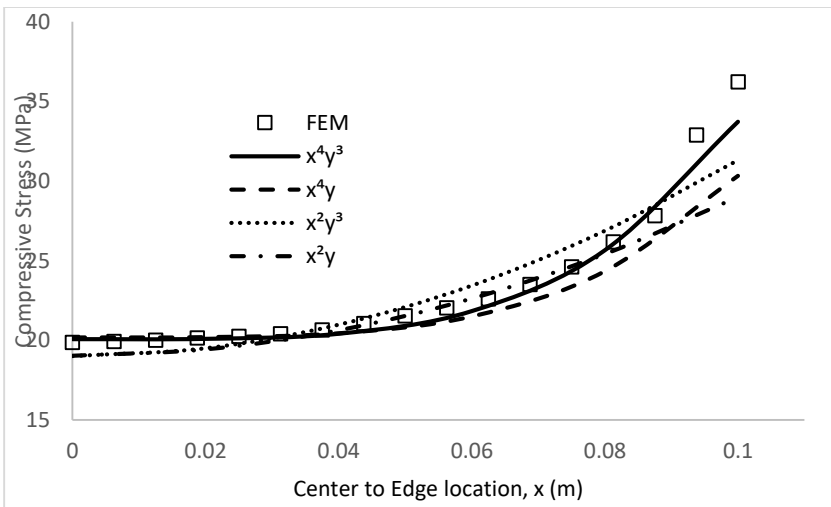

Figure 9: Fourth Comparison of Various Deplanation Functions, and FEM.

Discussion

The structure used in the first comparison had a small $\frac{t}{r_{avg}} \approx 0.030$ which satisfies the thin-walled structure definition. In comparing the analytical Stress-form Method's Deplanation functions with the experimental data, functions with quartic-x or x^4 provided the closest matches as opposed to quadratic-x or x^2, even though both of them slightly underestimated at most of the central part. However, the function $\overline{\varphi_4} = x^4y^3$, i.e. a combination of quartic-x and cubic-y function provides the best match combination of the experimental data curve as well as the FEM results near the edge part. It is interesting to note that the characteristic of the functions with quartic-x or x^4 of having almost flat variation in the center part enhances matching with the experimental data here. Moreover, the characteristic of the function with cubic-y or y^3 having steeper slopes enhances matching with the FEM results at the edge. Important to note that in contrast, the classical deplanation function was $\overline{\varphi_4} = x^2y$ as used in [1, 3].

The structure used in the second comparisons had a relatively large $\frac{t}{r_{avg}} \approx 0.107$ which also does not satisfy the thin-walled structure definition. In comparing the analytical Stress-form Method Deplanation functions with the experimental data, again functions with quartic-x or x^4 provided better matches as opposed to quadratic-x or x^2, even though in this case both of them slightly overestimated at some of the parts but also significantly at other parts especially with respect to the function $\overline{\varphi_4} = x^4y^3$. However, the function $\overline{\varphi_4} = x^4y$, i.e. a combination of quartic-x and linear-y function provides a better combined match for both the experimental data curve and FEM results.

Overall, the comparison of the second structure showed less satisfactory matching because it does not satisfy the thin-walled structure definition and probably the measured experimental data have significant errors. Figure 10 compares the differences of stresses from the FEM results between the outside and inside surfaces of both structures. Here it is observed that in the second structure, the difference of the stresses on the inside and the outside surfaces is significant in comparison to the first structure. As a result, the second structure cannot be considered a thin-walled structure.

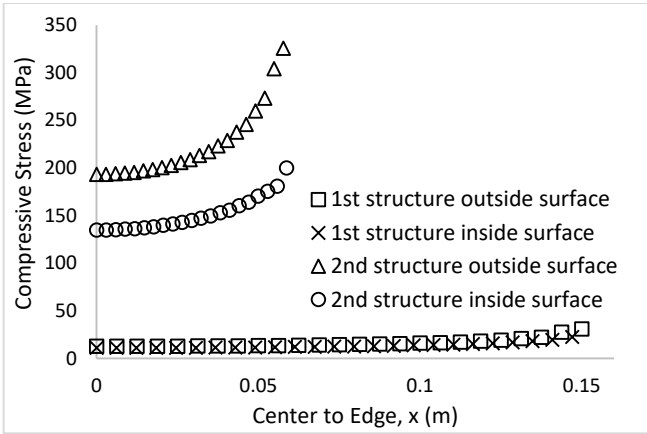

Figure 10: FEM results between outside and inside surfaces of both structure's flanges.

The structure used in the third and fourth comparisons had $\frac{t}{r_{avg}} \approx 0.024$ and $\frac{t}{r_{avg}} \approx 0.04$, respectively, which satisfy the thin-walled structure definition. No experimental data were available, however, as in the first comparison, the Deplanation function $\overline{\varphi_4} = x^4y^3$, i.e. a combination of quartic-x and cubic-y function provides the best match with FEM results.

Conclusion

Based on the comparative study done in this paper, the developed Stress-form analytical method for calculation of stresses discovered two significant findings. Primarily, the quartic variant deplanation functions were shown to produce improved matching to experimental results as compared to the classical quadratic one. Secondarily, only structures that conform to the definition of a thin-walled structure yield good results. Noteworthy to point out that the characteristic of the functions with quartic-x or x^4 of having almost flat variation in the center part enhances matching with the experimental data. Moreover, the characteristic of the function with cubic-y or y^3 having steeper slopes enhances matching with the FEM results at the edge.

Acknowledgments

Both Universiti Sains Malaysia (USM) Research University Grant RU814042 and USM Post-Graduate Incentive Grant funded this study.

References

[1] A. H. Kadarman, S. Shuib, A. H. Hassan, M. A. I. A. Zahrol, "Thin-walled Box Beam Bending Distortion Analytical Analysis", *Journal of Mechanical Engineering*, 14 (1). pp 1-17, 2017.

[2] V. Z.V lasov, *Thin-Walled Elastic Beams*, 2nd ed., State Publishing of Physics-Mathematical Literature, (in Russian), Moscow, 1959.

[3] MAPLE 18, Waterloo Maple Inc. (Maple Soft), 2018.

[4] I. F. Obraztsov, , L. A. Bulychev, V.V. Vasilev et al., "Mechanics of Building Flying Vehicles", Machine-building Publishing, (in Russian), Moscow, 1986.

[5] Zhibin Lin, Jian Zhao, "Least-work solutions of flange normal stresses in thin-walled flexural members with high-order polynomials", *Engineering Structures*, vol. 33, pp 2759-2760, 2011.

[6] Jun Chen, Shui-Long Shen, Zhen-Yu Yin, and Suksun Horpibulsuk, "Closed-form solution for shear lag with derived flange deformation function", *Journal of Constructional Steel Research*, vol. 102, pp 104-110, 2014.

[7] Zhibin Lin, Jian Zhao, "Modeling Inelastic Shear Lag in Steel Box Beams", Engineering Structures, vol. 41, pp 90-97, 2012.

[8] V. Kristek, H.R. Evan, M.K.M. Ahmad, "A shear lag analysis for composite box girders", *J Constr Steel Res*, vol. 16, no. 1, pp 16. 1990.

[9] A. A. Dudchenko, Building Mechanics of Composite Space Design, Educational text, Moscow Aviation Institute Publishing, (in Russian), Moscow, 1997.

[10] O. A. Bauchau, J. I. Craig, "Structural Analysis: With Applications to Aerospace Structures," Springer, Dordrecht Heidelberg London New York, pp 308, 2009.

[11] C. F. Kollbrunner, K. Basler, "Torsion in Structures: An Engineering Approach," Springer Science & Business Media, pp 3,123, 2013.

[12] E. Ventsel, and T. Krauthammer, "Thin Plates and Shells Theory, Analysis, and Applications," Marcel Dekker, Inc, New York, 2001.

[13] D. F. Griffiths, J. W. Dold, and D. J. Silvester, "Essential Partial Differential Equations: Analytical and Computational Aspects," Springer, Switzerland, 2015.

[14] F. Rindler, Calculus of Variations, Springer International Publishing AG, part of Springer Nature, 2018.

[15] P. Bertolinia, M.A. Eder, L. Taglialegne, P.S. Valvo, "Stresses in constant tapered beams with thin-walled rectangular and circular cross sections," Thin-Walled Structures, 2019.

[16] SOLIDWORKS 2019 Education Edition, Dassault Systemes, 2019.

[17] D. H. Allen & W. E. Haisler, "Introduction to Aerospace Structural Analysis", John Wiley & Sons, pp 190, 1985.

Nomenclatures

E, G	= modulus of elasticity and rigidity of thin walled panel, respectively
μ	= poisson ratio
x, y, z	= dimensional coordinates with respect to width, height and length of the thin panel beam
s	= curvilinear coordinates with respect to the contour of the thin panel
w_y	= distributed load in y-direction
V_y	= transversal shear force in the y-direction
M_x	= flexural bending about axis x
M_z	= torsional twisting about axis z
N_z, N_s, N_{zs}	= stress resultants in thin panel, force per unit length
r	= r-th panel
h_r	= thickness of the panel of the corresponding r-th panel
t	= thickness of the uniform thickness box beam
r_{avg}	= average radius
l_r	= length along the contour of the r-th panel
ρ	= moment-arm of the shear flow q about axis z
ω	= double of area of the analyzed contour
$\overline{\varphi_4}$	= deplanation function

Appendix

Self-equilibrium coefficient is the same as the coefficient of orthogonalization. Here, orthogonal means: Any two nontrivial functions u(x) and v(x) are said to be orthogonal if

$$<u,v> = \int u \cdot v \, dx = 0$$

The special characteristic of this concept is described in [4] whereby using the orthogonalization process the function $\overline{\varphi_3}(s)$ in Figure A1.1 can be balanced or self-equilibrium to be $\varphi_3(s)$ as in Figure A1.2 where essentially the area above and below the horizontal axis is the same and if integration of $\varphi_3(s)$ is taken, the result will be zero.

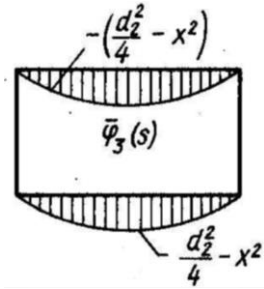

Figure A1: Deplanation function, $\overline{\varphi_3}$(s) [4]

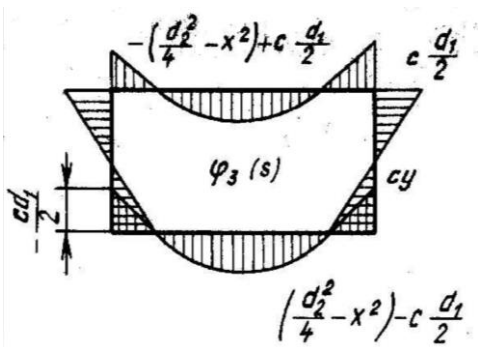

Figure A2: Balanced or self-equilibrium, φ_3(s) [4]